J|A|C|S
COMMUNICATIONS

Published on Web 03/12/2004

Structural Characterization of a Pentacene Monolayer on an Amorphous SiO_2 Substrate with Grazing Incidence X-ray Diffraction

Sandra E. Fritz,[†] Stephen M. Martin,[†] C. Daniel Frisbie,*,[†] Michael D. Ward,*,[†] and Michael F. Toney*,[‡]

Department of Chemical Engineering and Materials Science, University of Minnesota, 421 Washington Avenue SE, Minneapolis, Minnesota 55455, and Stanford Synchrotron Radiation Laboratory, Stanford Linear Accelerator Center, 2575 Sand Hill Road, M/S 69, Menlo Park, California 94025

Received January 15, 2004; E-mail: wardx004@umn.edu; frisbie@cems.umn.edu; mftoney@slac.stanford.edu

Pentacene, a simple linear oligoacene consisting of five fused benzene rings, has emerged as a viable candidate for the semiconducting transport layer in organic thin film transistors (OTFTs).[1−4] The interest in pentacene films, which exhibit p-type transport, primarily stems from their relatively high hole mobilities and high on-to-off current ratios in OTFTs.[5] Carrier transport in the channel between the source and drain electrodes is thought to occur in the first few layers of the semiconductor, or perhaps the first layer, in proximity with the dielectric layer adjacent to the gate electrode.[6,7] It is also widely recognized that the transport properties of crystalline organic films depend strongly on the intermolecular overlap of electronic wave functions within the semiconductor layer, which is very sensitive to the molecular packing in the crystal.[8,9] Surprisingly, little is known about the detailed crystal structure of the active transport layers in OTFTs, including pentacene films. We report herein preliminary grazing-angle incidence X-ray diffraction (GIXD) data for a monolayer-thick pentacene film grown on amorphous silicon dioxide (a-SiO_2), a commonly used dielectric layer in OTFTs. The data confirm that the monolayer is crystalline and has a structure that differs from that of bulk pentacene, which has important implications for carrier transport in pentacene-based OTFTs.

The crystal structure of bulk pentacene consists of layers of pentacene molecules arranged in a herringbone packing motif with an interlayer spacing of $d_{001} = 14.1$ Å.[10,11] Three "thin film" multilayer phases with different d_{001} values of 14.4, 15.0, and 15.4 Å have been identified by wide-angle X-ray diffraction.[12,13] The selectivity toward these multilayer phases appears to be governed by a variety of factors including substrate material, substrate temperature during deposition, rate of deposition, and film thickness.[12,14,15] The different d_{001} values imply dissimilar packing of the pentacene molecules in the *ab* plane, which is regarded as the high-mobility plane for hole transport in pentacene-based OTFTs. Despite its importance to transport, structural characterization of the *ab* plane in the multilayer phases has been limited to substrates other than a-SiO_2,[12,13,16−18] and the crystal structure of a pentacene monolayer on any substrate, including a-SiO_2, has not been reported.

Atomic force microscopy (AFM) of a vacuum sublimed pentacene monolayer[19] on a-SiO_2 reveals micrometer-sized domains with a thickness of 16.0 ± 0.6 Å (Figure 1).[20] Characterization of this pentacene monolayer by GIXD at room temperature[21] afforded a diffraction pattern (Figure 2) that could be indexed to a near-rectangular in-plane unit cell with dimensions $a = 5.916$ Å, $b = 7.588$ Å, and $\gamma = 89.95°$. These values differ from the corresponding lattice parameters reported for bulk pentacene ($a = 6.266$ Å, $b = 7.775$ Å, and $\gamma = 84.684°$), but are consistent with a packing motif resembling the (001) layers in the bulk form, that is, with the pentacene molecules in the monolayer adopting a near-vertical orientation on the a-SiO_2 substrate. The diffraction peaks were very narrow, consistent with crystallite sizes >70 nm and in agreement with the large domains observed by AFM. The peak widths increase with increasing q_{xy} beyond that expected from Debye−Scherrer broadening, suggesting small variations in the in-plane d-spacings of the crystallites.[22] A broad feature centered at $q_{xy} = 1.55$ Å^{-1} is due to the amorphous SiO_2 substrate.

A model of the monolayer structure was constructed using the room-temperature single-crystal structure of bulk pentacene as a

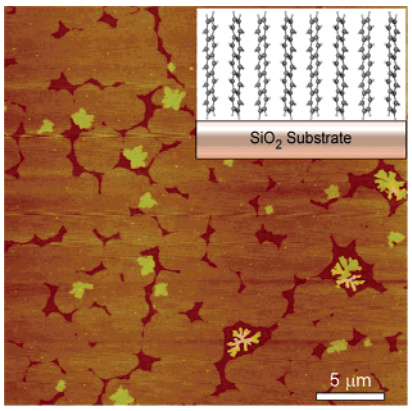

Figure 1. A tapping-mode AFM image, acquired in air under ambient conditions, of monolayer-thick pentacene domains on a 3000 Å thick a-SiO_2 film. Inset: Pentacene monolayer structure based on GIXD.

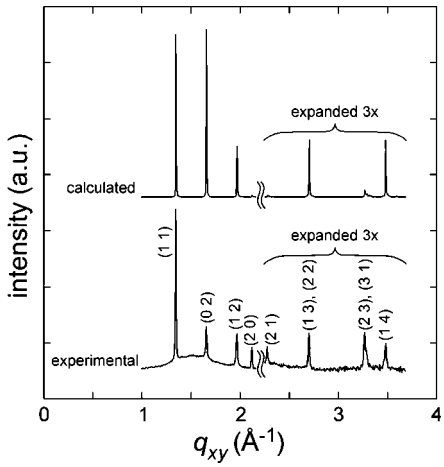

Figure 2. GIXD pattern (bottom) for a pentacene monolayer and a diffraction pattern (top) calculated for an energy-minimized crystal structure model based on the GIXD lattice parameters and the (001) layer motif of bulk pentacene as the starting point.

[†] University of Minnesota.
[‡] Stanford Linear Accelerator Center.

10.1021/ja049726b CCC: $27.50

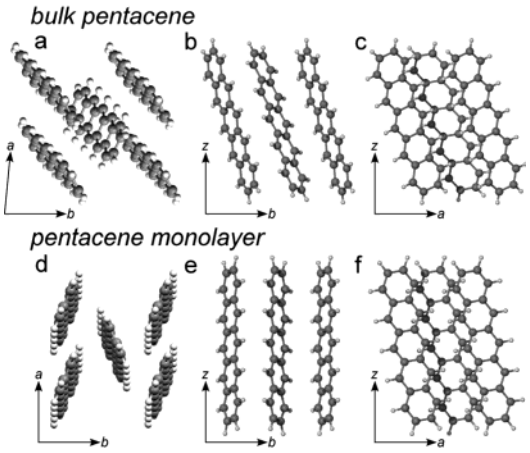

Figure 3. Normal views of the *ab* planes of bulk pentacene and the model monolayer structures (left) and the respective side views (center, right). The *z*-axis is the normal to the *ab* plane.

starting point. The *a* and *b* lattice parameters of the bulk structure were adjusted to the monolayer values, and the interlayer d_{001} spacing was expanded to an arbitrarily large distance (800 Å) to mimic an isolated monolayer. The lowest energy monolayer structure (ignoring contributions from the substrate) was then determined using the universal force field within the Cerius[2] environment (Accelrys).[23] The diffraction pattern produced by this energy-minimized monolayer structure is in reasonable agreement with the GIXD data, although the integrated intensities for some of the diffraction peaks for the preliminary model structure differ from those observed experimentally, particularly the relative intensities of the (11) and (02) peaks. Some of the discrepancy can be attributed to contributions from the *a*-SiO_2 background, particularly in the lower q_{xy} region. We anticipate that a more complete data set, particularly data collected at $q_z > 0$, will permit precise determination of the pentacene tilt and an improved refinement of the crystal structure.[24] Nevertheless, the GIXD data demonstrate unequivocally that the pentacene monolayer on the *a*-SiO_2 dielectric layer is highly crystalline and has a structure that is distinguishable from the bulk.

The energy-minimized monolayer structure exhibits a herringbone packing of the pentacene molecules similar to that observed in the bulk (Figure 3). The herringbone "edge-to-face" angle between pentacene molecules is 48.1°, as compared to 52.3° angle in bulk pentacene. The pentacene molecules in the bulk phase tilt 25.1° with respect to the surface normal (*z*) along an azimuthal angle of 139.7° (clockwise) with respect to the *a* axis. In contrast, the pentacene molecules in the model structure are tilted along the *a* axis by 11° with respect to *z*, and the tilt along the *b* axis is negligible. On the basis of this tilt and an estimated length of ca. 16.4 Å for the pentacene molecule, the anticipated monolayer thickness is 16.1 Å, in good agreement with the thickness measured by AFM.

These results demonstrate that a pentacene monolayer film on *a*-SiO_2 − the dielectric layer often used in OTFTs − is highly crystalline and has a structure that differs from the (001) layers in single crystals of bulk pentacene. The structural parameters of the monolayer also differ from most previously reported multilayers, although they are near those reported recently for pentacene multilayer films on a (100) NaCl substrate (by TEM).[18] GIXD is uniquely suited for unraveling the structure−property relationships associated with carrier transport in these films because it can probe the region near the dielectric layer where transport most likely occurs. Furthermore, GIXD can be used to characterize films on various substrates and during application of gate bias, providing much-needed insight into the factors governing performance of OTFTs under actual operating conditions.

Acknowledgment. This work was supported primarily by the MRSEC Program of the National Science Foundation under Award Number DMR-0212302. Research was carried out in part at the National Synchrotron Light Source, Brookhaven National Laboratory, which is supported by the U.S. Department of Energy, Division of Materials Sciences and Division of Chemical Sciences, under Contract No. DE-AC02-98CH10886. Portions of this research were carried out at the Stanford Synchrotron Radiation Laboratory, a national user facility operated by Stanford University on behalf of the U.S. Department of Energy, Office of Basic Energy Sciences. Computational resources were provided by the Minnesota Supercomputing Institute Scientific Computing and Visualization Laboratory.

References

(1) Lin, Y.-Y.; Gundlach, D. J.; Nelson, S. F.; Jackson, T. N. *IEEE Electron Device Lett.* **1997**, *18*, 606.
(2) Dimitrakopoulos, C. D.; Malenfant, P. R. L *Adv. Mater*. **2002**, *14*, 99.
(3) Karl, N. *Synth. Met.* **2003**, *133*−*134*, 649.
(4) Horowitz, G. *Adv. Mater*. **1998**, *10*, 365.
(5) Baude, P. F.; Ender, D. A.; Haase, M. A.; Kelley, T. W.; Muyres, D. V.; Theisse, S. D. *Appl. Phys. Lett.* **2003**, *82*, 3964.
(6) Dodabalapur, A.; Torsi, L.; Katz, H. E. *Science* **1995**, *268*, 270.
(7) Granstrom, E. L.; Frisbie, C. D. *J. Phys. Chem*. **1999**, *103*, 8842.
(8) Cornil, J.; Calbert, J. Ph.; Bredas, J. L. *J. Am. Chem. Soc.* **2001**, *123*, 1250.
(9) Cheng, Y. C.; Silbey, R. J.; da Silva Filho, D. A.; Calbert, J. P.; Cornil, J.; Bredas, J. L. *J. Chem. Phys.* **2003**, *118*, 3764.
(10) Holmes, D.; Kumaraswamy, S.; Matzger, A. J.; Vollhardt, K. P. C. *Chem.-Eur. J.* **1999**, *5*, 3399.
(11) Mattheus, C. C.; Dros, A. B.; Baas, J.; Meetsma, A.; de Boer, J. L.; Palstra, T. T. M. *Acta Crystallogr*. **2001**, *C57*, 939.
(12) Mattheus, C. C.; Dros, A. B.; Baas, J.; Oostergetel, G. T.; Meetsma, A.; de Boer, J. L.; Palstra, T. M. *Synth. Met.* **2003**, *138*, 475.
(13) Minakata, T.; Imai, H.; Ozaki, M.; Saco, K. *J. Appl. Phys.* **1992**, *72*, 5220.
(14) Bouchoms, I. P. M.; Schoonveld, W. A.; Vrijmoeth, J.; Klapwijk, T. M. *Synth. Met.* **1999**, *104*, 175.
(15) Knipp, D.; Street, R. A.; Volkel, A.; Ho, J. *J. Appl. Phys.* **2003**, *93*, 347.
(16) The *ab* lattice parameters for the 15.0 and 15.4 Å phases were surmised from electron diffraction of individual microcrystals without simultaneous determination of d_{001}, precluding an unequivocal assignment.
(17) Drummy, L. F.; Kubel, C.; Lee, D.; White, A.; Martin, D. C. *Adv. Mater*. **2002**, *14*, 54.
(18) Wu, J. S.; Spence, J. C. H. *J. Appl. Crystallogr*. **2004**, *37*, 78.
(19) Pentacene monolayers were deposited at 0.02 Å/s by vacuum sublimation (10^{-7} Torr) onto an amorphous-SiO_2 layer grown by thermal oxidation of a heavily doped ⟨100⟩ oriented silicon wafer. Pentacene was purified by gradient sublimation prior to vacuum sublimation of films.
(20) Pentacene monolayers on a variety of substrates, some with different pentacene orientations, have been characterized by other methods: (a) Meyer zu Hereingdorf, F.-J.; Reuter, M. C.; Tromp, R. M. *Nature* **2001**, *412*, 517. (b) Schroeder, P. G.; France, C. B.; Park, J. B.; Parkinson, B. A. *J. Appl. Phys.* **2002**, *91*, 3010. (c) Ruiz, R.; Nickel, B.; Koch, N.; Feldman, L. C.; Haglund, R. F.; Kahn, A.; Scoles, G. *Phys. Rev. B* **2003**, *67*, 125406.
(21) GIXD was performed at the National Synchrotron Light Source (NSLS), using beamline X20C at an incident angle of 0.25° and an X-ray energy of 7.0 keV.
(22) Snyder, R. L., Fiala, J.; Bunge, H. J. *Defect and Microstructure Analysis by Diffraction*; Oxford: New York, 1999.
(23) The energy-minimized structure was independent of the initial orientation of the pentacene molecules in the unit cell as well as the convergence method used during the minimization (i.e., the Cerius[2] "Smart Minimizer", steepest descent, Newton−Raphson).
(24) Kuzmenko, I.; Rapaport, H.; Kjaer, K.; Als-Nielsen, J.; Weissbuch, I.; Lahav, M.; Leiserowitz, L. *Chem. Rev.* **2001**, *101*, 1659.

JA049726B